Non-linear dynamics in damping rings

Yannis PAPAPHILIPPOU
Accelerator and Beam Physics group
Beams Department
CERN

Eighth International Accelerator School for Linear Colliders
4-15 December 2013, Antalya

Outline

- Gradient error
- Chromaticity and correcting sextupoles
- Perturbation of Hills equation
- Resonance conditions and tune-spread
- Non-linear dynamics due to sextupoles and multipoles
- Chaotic motion and Dynamic aperture
- Frequency map analysis

Gradient error

- Consider the transfer matrix for 1-turn

$$\mathcal{M}_0 = \begin{pmatrix} \cos(2\pi Q) + \alpha_0 \sin(2\pi Q) & \beta_0 \sin(2\pi Q) \\ -\gamma_0 \sin(2\pi Q) & \cos(2\pi Q) - \alpha_0 \sin(2\pi Q) \end{pmatrix}$$

- Consider a gradient error in a quad. In thin element approximation the quad matrix with and without error are

$$m_0 = \begin{pmatrix} 1 & 0 \\ -K_0(s)ds & 1 \end{pmatrix} \text{ and } m = \begin{pmatrix} 1 & 0 \\ -(K_0(s) + \delta K)ds & 1 \end{pmatrix}$$

- The new 1-turn matrix is $\mathcal{M} = m m_0^{-1} \mathcal{M}_0 = \begin{pmatrix} 1 & 0 \\ -\delta K ds & 1 \end{pmatrix} \mathcal{M}_0$ which yields

$$\mathcal{M} = \begin{pmatrix} \cos(2\pi Q) + \alpha_0 \sin(2\pi Q) & \beta_0 \sin(2\pi Q) \\ \delta K ds(\cos(2\pi Q) - \alpha_0 \sin(2\pi Q)) - \gamma_0 \sin(2\pi Q) & \cos(2\pi Q) - (\delta K ds \beta_0 + \alpha_0) \sin(2\pi Q) \end{pmatrix}$$

Gradient error and tune-shift

- Consider a new matrix after 1 turn with a new tune $\chi = 2\pi(Q + \delta Q)$

$$\mathcal{M}^\star = \begin{pmatrix} \cos(\chi) + \alpha_0 \sin(\chi) & \beta_0 \sin(\chi) \\ -\gamma_0 \sin(\chi) & \cos(\chi) - \alpha_0 \sin(\chi) \end{pmatrix}$$

- The traces of the two matrices describing the 1-turn should be equal $\quad \mathrm{Tra}(\mathcal{M}^\star) = \mathrm{Tra}(\mathcal{M})$

  which gives $\;2\cos(2\pi Q) - \delta K ds \beta_0 \sin(2\pi Q) = 2\cos(2\pi(Q + \delta Q))$

- Developing the left hand side

$$\cos(2\pi(Q + \delta Q)) = \cos(2\pi Q) \underbrace{\cos(2\pi\delta Q)}_{1} - \sin(2\pi Q) \underbrace{\sin(2\pi\delta Q)}_{2\pi\delta Q}$$

  and finally $\;4\pi\delta Q = \delta K ds \beta_0$

- For a quadrupole of finite length, we have

$$\delta Q = \frac{1}{4\pi} \int_{s_0}^{s_0+l} \delta K \beta_0 ds$$

Gradient error and beta distortion

- Consider the unperturbed transfer matrix for one turn

$$M_0 = \begin{pmatrix} m_{11} & m_{12} \\ m_{21} & m_{22} \end{pmatrix} = B \cdot A \quad \text{with} \quad A = \begin{pmatrix} a_{11} & a_{12} \\ a_{21} & a_{22} \end{pmatrix} \quad B = \begin{pmatrix} b_{11} & b_{12} \\ b_{21} & b_{22} \end{pmatrix}$$

- Introduce a gradient perturbation between the two matrices

$$\mathcal{M}_0^\star = \begin{pmatrix} m_{11}^\star & m_{12}^\star \\ m_{21}^\star & m_{22}^\star \end{pmatrix} = B \begin{pmatrix} 1 & 0 \\ -\delta K ds & 1 \end{pmatrix} A$$

- Recall that $m_{12} = \beta_0 \sin(2\pi Q)$ and write the perturbed term as

$$m_{12}^\star = (\beta_0 + \delta\beta)\sin(2\pi(Q + \delta Q)) = m_{12} + \delta\beta \sin(2\pi Q) + 2\pi\delta Q \beta_0 \cos(2\pi Q)$$

where we used $\sin(2\pi\delta Q) \approx 2\pi\delta Q$ and $\cos(2\pi\delta Q) \approx 1$

Gradient error and beta distortion

- On the other hand

$$a_{12} = \sqrt{\beta_0\beta(s_1)}\sin\psi,\;\; b_{12} = \sqrt{\beta_0\beta(s_1)}\sin(2\pi Q - \psi)$$

and $m^{\star}_{12} = \underbrace{b_{11}a_{12} + b_{12}a_{22}}_{m_{12}} - a_{12}b_{12}\delta K ds = m_{12} - a_{12}b_{12}\delta K ds$

- Equating the two terms

$$\delta\beta\sin(2\pi Q) + 2\pi\delta Q\beta_0\cos(2\pi Q) = \; - a_{12}b_{12}\delta K ds$$

- Integrating through the quad

$$\frac{\delta\beta}{\beta_0} = -\frac{1}{2\sin(2\pi Q)}\int_{s_1}^{s_1+l}\beta(s)\delta K(s)\cos(2\psi - 2\pi Q)ds$$

Chromaticity

- Linear equations of motion depend on the energy (term proportional to dispersion)
- Chromaticity is defined as: $\xi_{x,y} = \frac{\delta Q_{x,y}}{\delta p/p}$
- Recall that the gradient is $k = \frac{G}{B\rho} = \frac{eG}{p} \rightarrow \frac{\delta k}{k} = \mp\frac{\delta p}{p}$
- This leads to dependence of tunes and optics function on energy
- For a linear lattice the tune shift is:

$$\delta Q_{x,y} = \frac{1}{4\pi}\oint \beta_{x,y}\delta k(s)ds = -\frac{1}{4\pi}\frac{\delta p}{p}\oint \beta_{x,y}k(s)ds$$

- So the **natural** chromaticity is:

$$\xi_{x,y} = -\frac{1}{4\pi}\oint \beta_{x,y}k(s)ds$$

- Sometimes the chromaticity is quoted as $\overline{\xi_{x,y}} = \frac{\xi_{x,y}}{Q_{x,y}}$

Chromaticity from sextupoles

- The sextupole field component in the *x*-plane is: $B_y = \frac{S}{2}x^2$
- In an area with non-zero dispersion $x = x_0 + D\frac{\delta P}{P}$
- Than the field is

$$B_y = \frac{S}{2}x_0^2 + \underbrace{SD\frac{\delta P}{P}x_0}_{\text{quadrupole}} + \underbrace{\frac{S}{2}D^2\frac{\delta P}{P}^2}_{\text{dipole}}$$

- Sextupoles introduce an equivalent focusing correction

$$\delta k = SD\frac{\delta P}{P}$$

- The sextupole induced chromaticity is

$$\xi^S_{x,y} = -\frac{1}{4\pi}\oint \mp\beta_{x,y}(s)S(s)D_x(s)ds$$

- The total chromaticity is the sum of the natural and sextupole induced chromaticity

$$\xi^{\rm tot}_{x,y} = -\frac{1}{4\pi}\oint \beta_{x,y}(s)\left(k(s) \mp S(s)D_x(s)\right)ds$$

Chromaticity correction

- Introduce sextupoles in high-dispersion areas
- Tune them to achieve desired chromaticity
- Two families are able to control horizontal and vertical chromaticity
- The off-momentum beta-beating correction needs additional families
- Sextupoles introduce non-linear fields (chaotic motion)
- Sextupoles introduce tune-shift with amplitude

Normalized coordinates

- Recall the Floquet solutions for betatron motion

$$u(s) = \sqrt{\epsilon\beta(s)}\cos(\psi(s)+\psi_0)$$

$$u'(s) = -\sqrt{\frac{\epsilon}{\beta(s)}}\left(\sin(\psi(s)+\psi_0)+\alpha(s)\cos(\psi(s)+\psi_0)\right)$$

- Introduce new variables

$$\mathcal{U} = \frac{u}{\sqrt{\beta}}\ ,\quad \mathcal{U}' = \frac{d\mathcal{U}}{d\phi} = \frac{\alpha}{\sqrt{\beta}}u + \sqrt{\beta}u'\ ,\quad \phi = \frac{\psi}{\nu} = \frac{1}{\nu}\int\frac{ds}{\beta(s)}$$

- In matrix form $\begin{pmatrix}\mathcal{U}\\ \mathcal{U}'\end{pmatrix} = \begin{pmatrix}\frac{1}{\sqrt{\beta}} & 0\\ \frac{\alpha}{\sqrt{\beta}} & \sqrt{\beta}\end{pmatrix}\begin{pmatrix}u\\ u'\end{pmatrix}$
- Hill's equation becomes $\frac{1}{\nu^2\beta^{3/2}}\left(\frac{d^2\mathcal{U}}{d\phi^2}+\nu^2\mathcal{U}\right) = 0$
- System becomes harmonic oscillator with frequency

$$\begin{pmatrix}\mathcal{U}\\ \mathcal{U}'\end{pmatrix} = \sqrt{\epsilon}\begin{pmatrix}\cos(\nu\phi)\\ -\sin(\nu\phi)\end{pmatrix} \quad \text{or} \quad \mathcal{U}^2 + \mathcal{U}'^2 = \epsilon$$

- **Floquet transformation** transforms phase space in circles

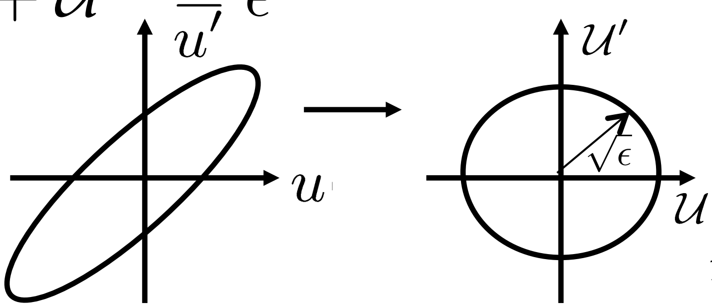

Perturbation of Hill's equations

- Hill's equations in normalized coordinates with harmonic perturbation, using $\mathcal{U} = \mathcal{U}_x$ or $\mathcal{U}_y$ and $\phi = \phi_x$ or ϕ_y

$$\frac{d^2\mathcal{U}}{d\phi^2} + \nu^2\mathcal{U} = \nu^2\beta^{3/2}F(\mathcal{U}_x(\phi_x),\mathcal{U}_y(\phi_y))$$

  where the *F* is the Lorentz force from perturbing fields
  - **Linear magnet imperfections**: deviation from the design dipole and quadrupole fields due to powering and alignment errors
  - **Time varying fields**: feedback systems (damper) and wake fields due to collective effects (wall currents)
  - **Non-linear magnets**: sextupole magnets for chromaticity correction and octupole magnets for Landau damping
  - **Beam-beam interactions**: strongly non-linear field
  - **Space charge effects**: very important for high intensity beams
  - **non-linear magnetic field imperfections**: particularly difficult to control for super conducting magnets where the field quality is entirely determined by the coil winding accuracy

Perturbation by periodic function

- In beam dynamics, perturbing fields are periodic functions
- The problem to solve is a generalization of the driven harmonic oscillator, $\frac{d^2u}{dt^2} + \omega_0^2 u(t) = g(t)$
  with a general periodic function $g(t)$, with frequency ω
- The right side can be Fourier analyzed: $g(t) = \sum_{m=-\infty}^{m=+\infty} a_m e^{im\omega t}$
- The homogeneous solution is $u_h(t) = u_0(t)\sin(\omega_0 t + \phi_0)$
- The particular solution can be found by considering that $u(t)$ has the same form as $g(t)$: $u_p(t) = \sum_{m=-\infty}^{m=+\infty} u_{pm} e^{im\omega t}$
- By substituting we find the following relation for the Fourier coefficients of the particular solution $u_{pm} = \frac{a_m}{\omega_0^2 - m^2\omega^2}$
- There is a **resonance condition** for infinite number of frequencies satisfying $\omega_0^2 = m^2\omega^2$

- For a generalized multi-pole perturbation, Hill's equation is:

$$\frac{d^2\mathcal{U}}{d\phi^2} + \nu_0^2\mathcal{U} = \nu_0^2\beta^{\frac{n}{2}+1}b_n(\phi)\mathcal{U}^{n-1} = \overline{b_n}(\phi)\mathcal{U}^{n-1}$$

- As before, the multipole coefficient can be expanded in Fourier series $\overline{b_n}(\phi) = \sum_{m=-\infty}^{\infty}\overline{b_{nm}}e^{im\phi}$
- Following the perturbation steps, the zero-order solution is given by the homogeneous equation $\mathcal{U}_0 = W_1e^{i\nu_0\phi} + W_{-1}e^{-i\nu_0\phi}$
- Then the position can be expressed as

$$\mathcal{U}_0^{n-1} = \sum_{k=0}^{n-1}\underbrace{\binom{n-1}{k}W_1^{n-1-k}W_{-1}^{k}}_{\overline{W}_q}e^{i\underbrace{(n-1-2k)}_{q}\nu_0\phi} = \sum_{q=-n+1}^{n-1}\overline{W}_q e^{iq\nu_0\phi}$$

$$q = -n+1, -n+3, \dots, n-1$$

with $\overline{W}_{n-2} = \overline{W}_{n-4} = \overline{W}_{n-6} = \cdots = \overline{W}_{-n+2} = 0$

- The first order solution is written as

$$\frac{d^2\mathcal{U}_1}{d\phi^2} + \nu_0^2\mathcal{U}_1 = \overline{b_n}(\phi)\mathcal{U}_0^{n-1} = \sum_{q=-n+1}^{n-1}\sum_{m=-\infty}^{m=\infty}\bar{b}_{nm}\overline{W}_q e^{i(m+q\nu_0)\phi}$$

Resonances for single multi-pole

- Following the discussion on the periodic perturbation, the solution can be found by setting the leading order solution to be periodic with the same frequency as the right hand side

$$\mathcal{U}_1 = \sum_{q=-n+1}^{n-1} \sum_{m=-\infty}^{m=\infty} \mathcal{U}_{1mq} e^{i(m+q\nu_0)\phi}$$

- Equating terms of equal exponential powers, the Fourier amplitudes are found to satisfy the relationship

$$\mathcal{U}_{1mq} = \frac{\bar{b}_{nm} \overline{W}_q}{\nu_0^2 - (m + q\nu_0)^2}$$

- This provides the **resonance condition** $m \pm |q|\nu_0 = \nu_0$ or $\nu_0 = \dfrac{m}{1 \pm |q|}$ which means that there are resonant frequencies for and "infinite" number of rationals

Tune-shift for single multi-pole

- Note that for even multi-poles and $q = 1$ or $m = 0$, there is a Fourier coefficient $\bar{b}_{n0}$, which is independent of ϕ and represents the average value of the periodic perturbation
- The perturbing term in the r.h.s. is

$$\bar{b}_{n0}\overline{W}_1 e^{i\nu_0\phi} = \nu_0^2 \beta^{\frac{n}{2}+1} b_{n0} \binom{n-1}{\frac{n}{2}-1} W_1^{n-1} W_{-1}^{\frac{n}{2}-1} e^{i\nu_0\phi}$$

which can be obtained for $k = \frac{n}{2} - 1$ (it is indeed an integer only for even multi-poles)

- Following the approach of the perturbed non-linear harmonic oscillator, this term will be secular unless a perturbation in the frequency is considered, thereby resulting to a tune-shift equal to

$$\delta\nu = -\frac{\nu_0 \beta^{\frac{n}{2}+1} b_{n0}}{2} \binom{n-1}{\frac{n}{2}-1} \widetilde{W}^{n-2} \quad \text{with} \quad \widetilde{W}^2 = W_1 W_{-1}$$

- This tune-shift is amplitude dependent for $n > 2$

Magnetic multipole expansion

- From Gauss law of magnetostatics, a vector potential exist

$$\nabla \cdot \mathbf{B} = 0 \quad \rightarrow \quad \exists \mathbf{A} : \quad \mathbf{B} = \nabla \times \mathbf{A}$$

- Assuming transverse 2D field, vector potential has only one component A_s. The Ampere's law in vacuum (inside the beam pipe) $\nabla \times \mathbf{B} = 0 \quad \rightarrow \quad \exists V : \quad \mathbf{B} = -\nabla V$
- Using the previous equations, the relations between field components and potentials are

$$B_x = -\frac{\partial V}{\partial x} = \frac{\partial A_s}{\partial y} \, , \quad B_y = -\frac{\partial V}{\partial y} = -\frac{\partial A_s}{\partial x}$$

i.e. Riemann conditions of an analytic function

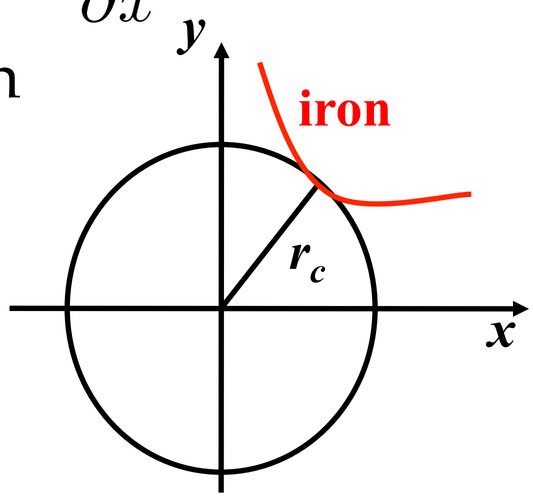

Exists complex potential of $z = x + iy$ with power series expansion convergent in a circle with radius $|z| = r_c$ (distance from iron yoke)

$$\mathcal{A}(x+iy) = A_s(x,y) + iV(x,y) = \sum_{n=1}^{\infty} \kappa_n z^n = \sum_{n=1}^{\infty} (\lambda_n + i\mu_n)(x+iy)^n$$

Multipole expansion II

- From the complex potential we can derive the fields

$$B_y + iB_x = -\frac{\partial}{\partial x}(A_s(x,y) + iV(x,y)) = -\sum_{n=1}^{\infty} n(\lambda_n + i\mu_n)(x+iy)^{n-1}$$

- Setting $b_n = -n\lambda_n \ , \quad a_n = n\mu_n$

$$B_y + iB_x = \sum_{n=1}^{\infty} (b_n - ia_n)(x+iy)^{n-1}$$

- Define normalized coefficients

$$b'_n = \frac{b_n}{10^{-4} B_0} r_0^{n-1} \ , \ a'_n = \frac{a_n}{10^{-4} B_0} r_0^{n-1}$$

on a reference radius r_0, 10^{-4} of the main field to get

$$B_y + iB_x = 10^{-4} B_0 \sum_{n=1}^{\infty} (b'_n - ia'_n)(\frac{x+iy}{r_0})^{n-1}$$

- **Note:** $n' = n - 1$ is the US convention

General multi-pole perturbation

- Equations of motion including any multi-pole error term, in both planes

$$\frac{d^2\mathcal{U}_x}{d\phi_x^2} + \nu_{0x}^2\mathcal{U}_x = \overline{b_{n,r}}(\phi_x)\mathcal{U}_x^{n-1}\mathcal{U}_y^{r-1}$$

- Expanding perturbation coefficient in Fourier series and inserting the solution of the unperturbed system on the rhs gives the following series:

$$\mathcal{U}_x^{n-1} \approx \mathcal{U}_{0x}^{n-1} = \sum_{q_x=-n+1}^{n-1} \overline{W}_{q_x} e^{iq_x\nu_0\phi_x}$$

$$\overline{b_{nr}}(\phi_x) = \sum_{m=-\infty}^{\infty} \overline{b_{nrm}} e^{im\phi_x}$$

$$\mathcal{U}_y^{r-1} \approx \mathcal{U}_{0y}^{r-1} = \sum_{q_y=-r+1}^{r-1} \overline{W}_{q_y} e^{iq_y\nu_{0y}\phi_x}$$

- The equation of motion becomes

$$\frac{d^2\mathcal{U}_x}{d\phi_x^2} + \nu_{0x}^2\mathcal{U}_x = \sum_{m,q_x,q_y} \overline{b_{nrm}} W_{q_x}^x W_{q_y}^y e^{i(m+q_x\nu_{0x}+q_y\nu_{0y})\phi_x}$$

- In principle, same perturbation steps can be followed for getting an approximate solution in both planes

General resonance conditions

- The general resonance conditions is $m + q_x \nu_{0x} + q_y \nu_{0y} = \nu_{0x}$ or $m + q'_x \nu_{0x} + q_y \nu_{0y} = 0$, with order $|q_x| + |q_y| + 1$
- The same condition can be obtained in the vertical plane
- For all the polynomial field terms of a $2n$-pole, the **main** excited resonances satisfy the condition $q'_x + q_y = n$ but there are also **sub-resonances** for which $q'_x + q_y < n$
- For **normal** (erect) multi-poles, the main resonances are $(q'_x, q_y) = (n, 0), \; (n-2, \pm 2), \ldots$ whereas for **skew** multi-poles $(q'_x, q_y) = (n-1, \pm 1), \; (n-3, \pm 3), \ldots$
- If perturbation is large, **all** resonances can be potentially excited
- The resonance conditions form lines in the frequency space and fill it up as the order grows (the rational numbers form a dense set inside the real numbers)

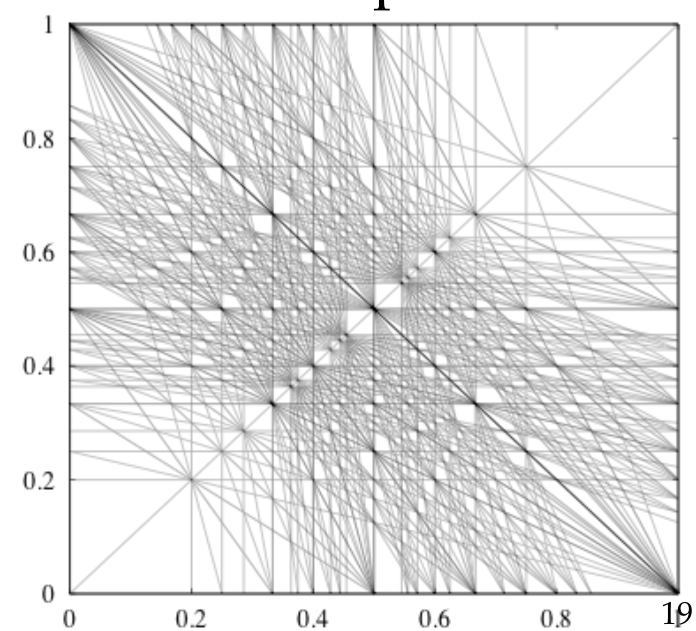

Systematic and random resonances

- If lattice is made out of N identical cells, and the perturbation follows the same periodicity, resulting in a reduction of the resonance conditions to the ones satisfying $q_x \nu_{0x} + q_y \nu_{0y} = jN$
- These are called **systematic** resonances
- Practically, any (linear) lattice perturbation breaks super-periodicity and any **random** resonance can be excited
- Careful choice of the working point is necessary

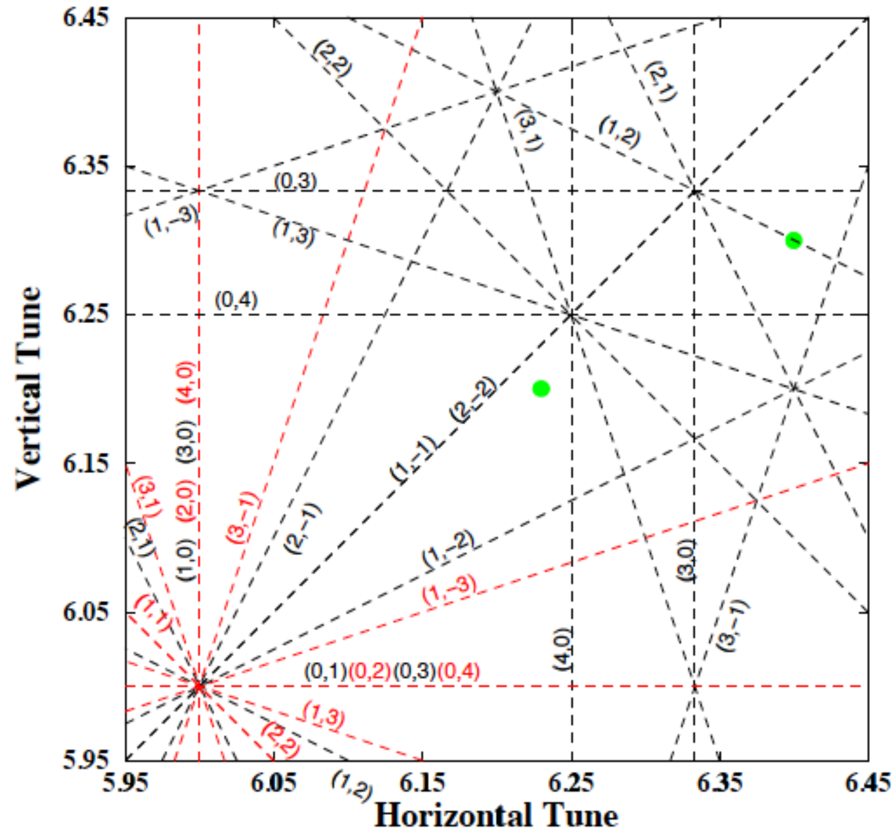

Fixed points for 3rd order resonance

- In the vicinity of a third order resonance, three fixed points can be found at

$$\psi_{20} = \frac{\pi}{3}, \ \frac{3\pi}{3}, \ \frac{5\pi}{3}, \quad J_{20} = \left(\frac{2\delta}{3A_{3p}}\right)^2$$

- For $\frac{\delta}{A_{3p}} > 0$ all three points are unstable
- Close to the elliptic one at $\psi_{20} = 0$ the motion in phase space is described by circles that they get more and more distorted to end up in the "triangular" separatrix uniting the unstable fixed points
- The tune separation from the resonance (**stop-band width**) is $\delta = \frac{3A_{3p}}{2} J_{20}^{1/2}$

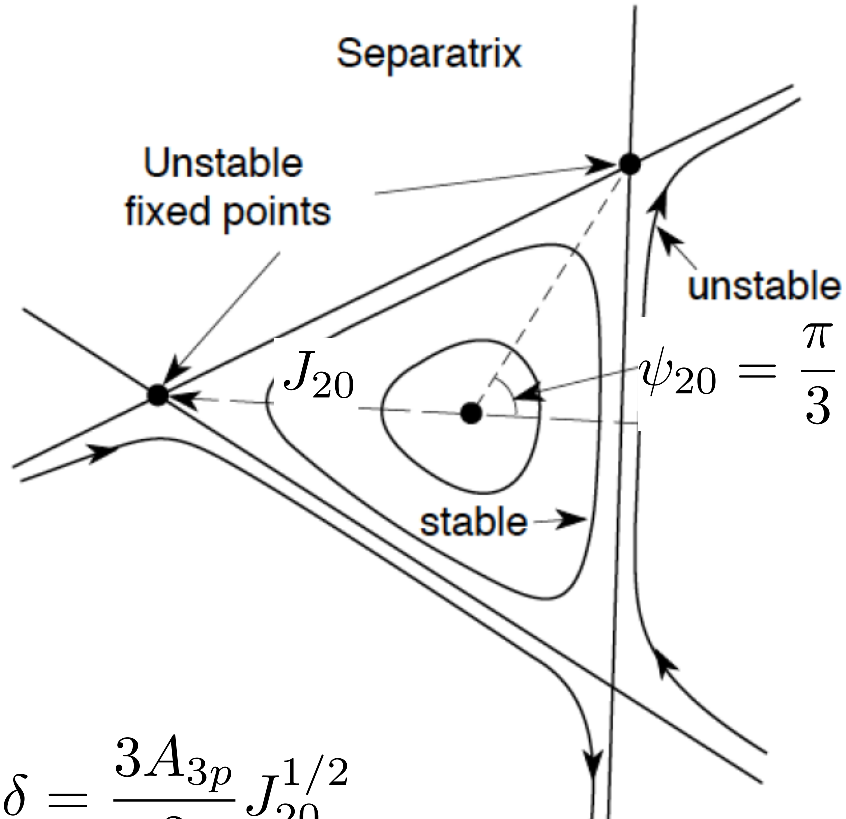

Topology of an octupole resonance

- Regular motion near the center, with curves getting more deformed towards a rectangular shape
- The separatrix passes through 4 unstable fixed points, but motion seems well contained
- Four stable fixed points exist and they are surrounded by stable motion (islands of stability)

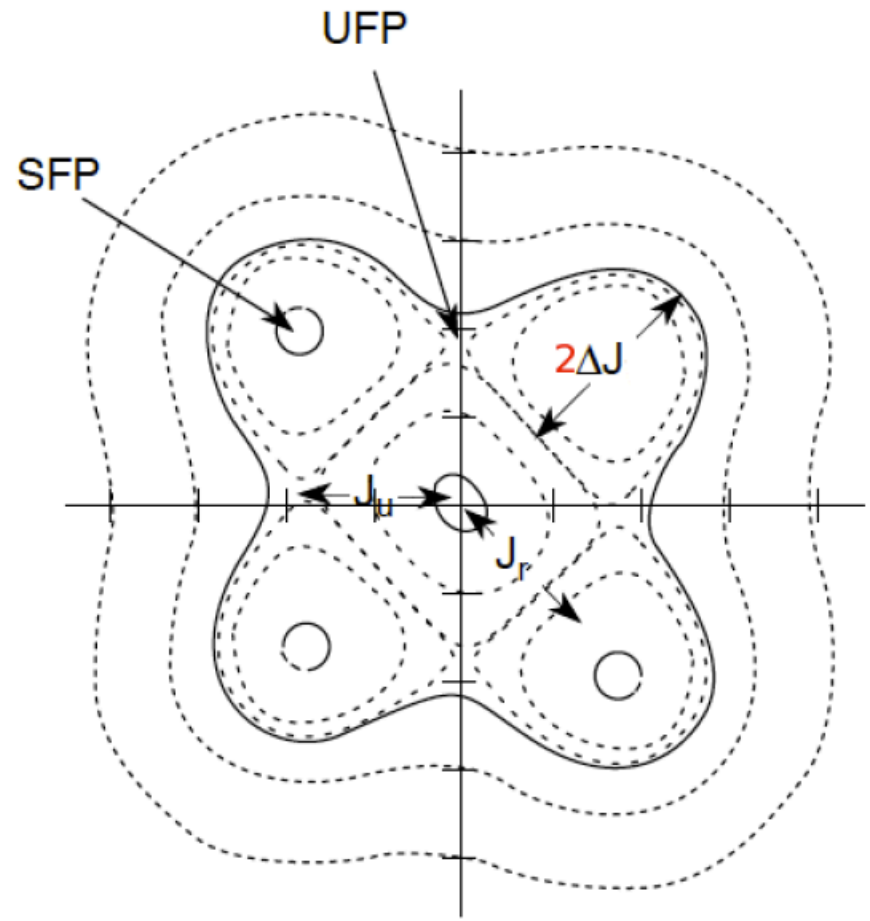

Path to chaos

- When perturbation becomes higher, motion around the separatrix becomes chaotic (producing tongues or splitting of the separatrix)
- Unstable fixed points are indeed the source of chaos when a perturbation is added

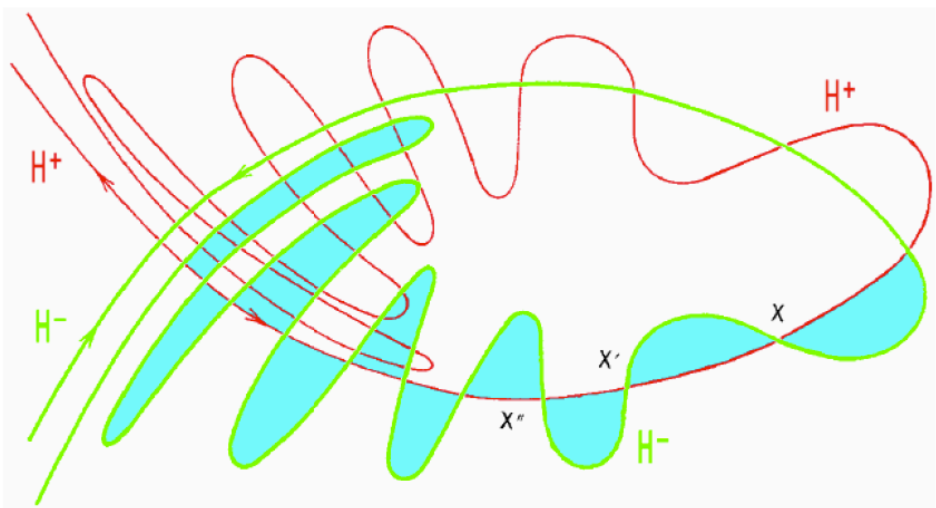

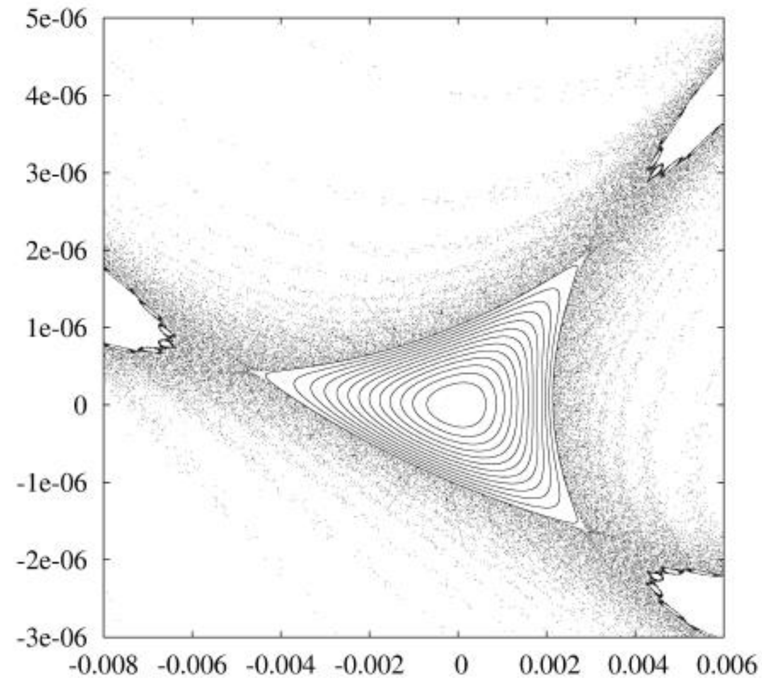

Chaotic motion

- Poincare-Birkhoff theorem states that under perturbation of a resonance only an even number of fixed points survives (half stable and the other half unstable)
- Themselves get destroyed when perturbation gets higher, etc. (self-similar fixed points)
- Resonance islands grow and resonances can overlap allowing diffusion of particles

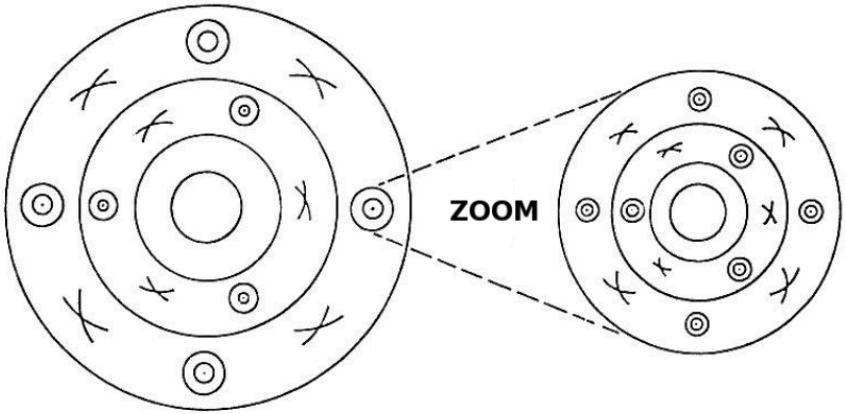

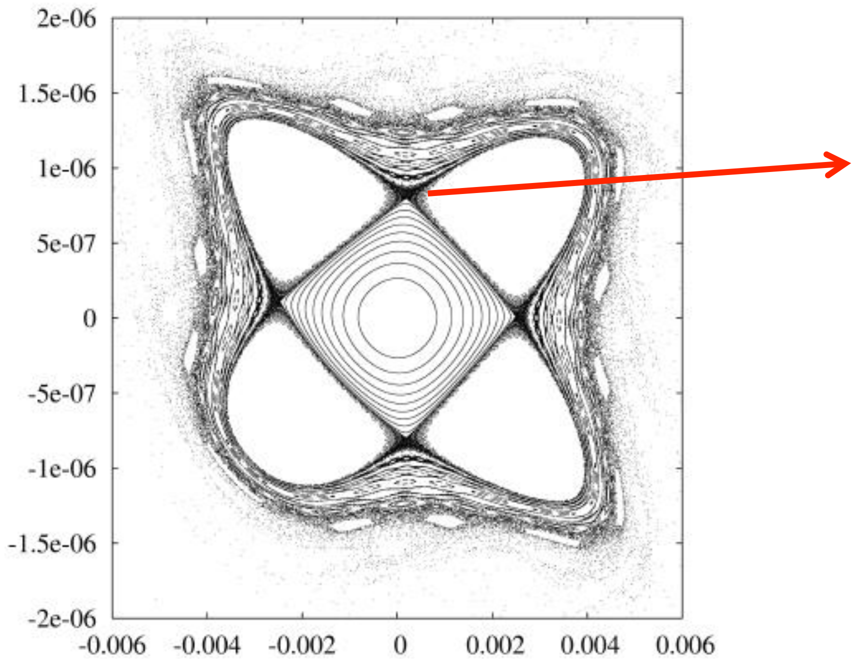

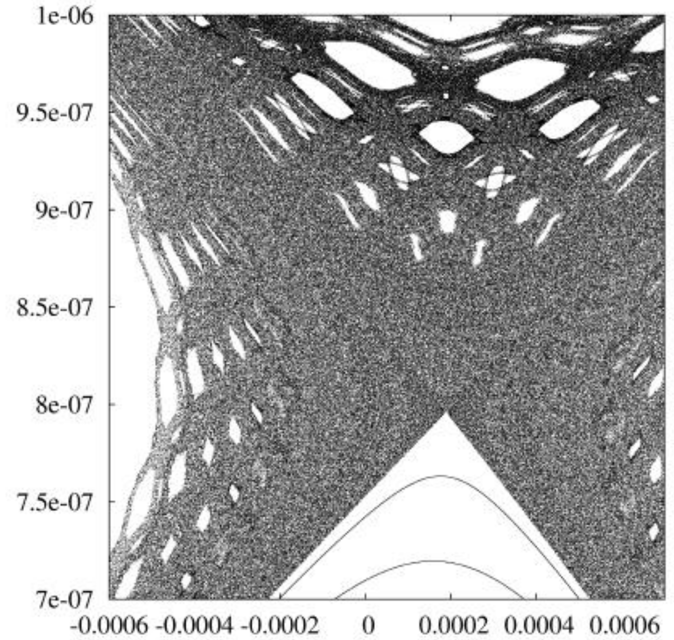

Beam Dynamics: Dynamic Aperture

- Dynamic aperture plots often show the maximum initial values of stable trajectories in x-y coordinate space at a particular point in the lattice, for a range of energy errors.
  - The beam size (injected or equilibrium) can be shown on the same plot.
  - Generally, the goal is to allow some significant margin in the design - the measured dynamic aperture is often significantly smaller than the predicted dynamic aperture.
- This is often useful for comparison, but is not a complete characterization of the dynamic aperture: a more thorough analysis is needed for full optimization.

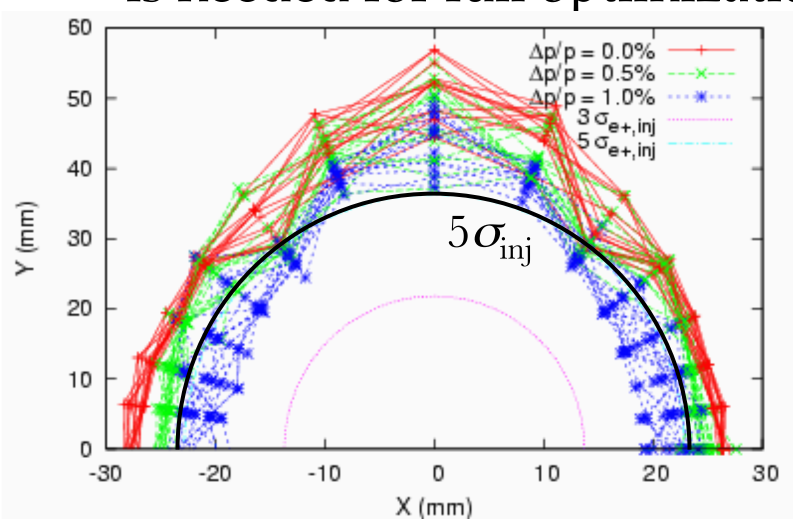

OCS: Circular TME

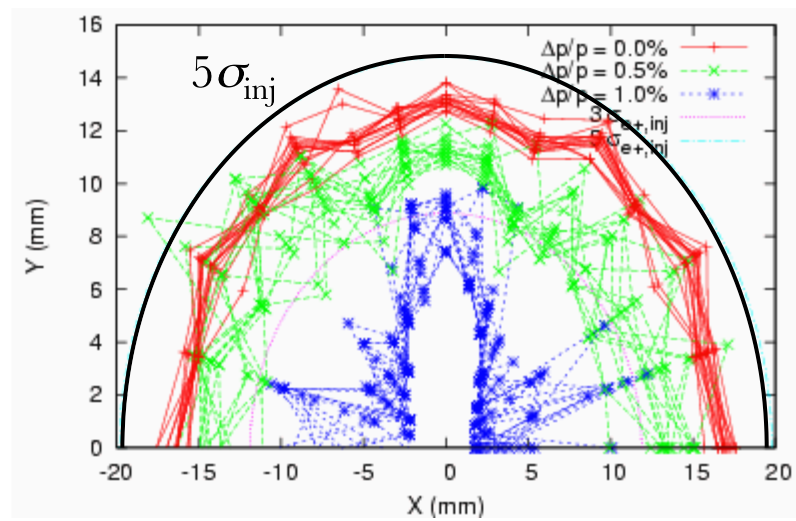

TESLA: Dogbone TME

Example: The ILC DR DA

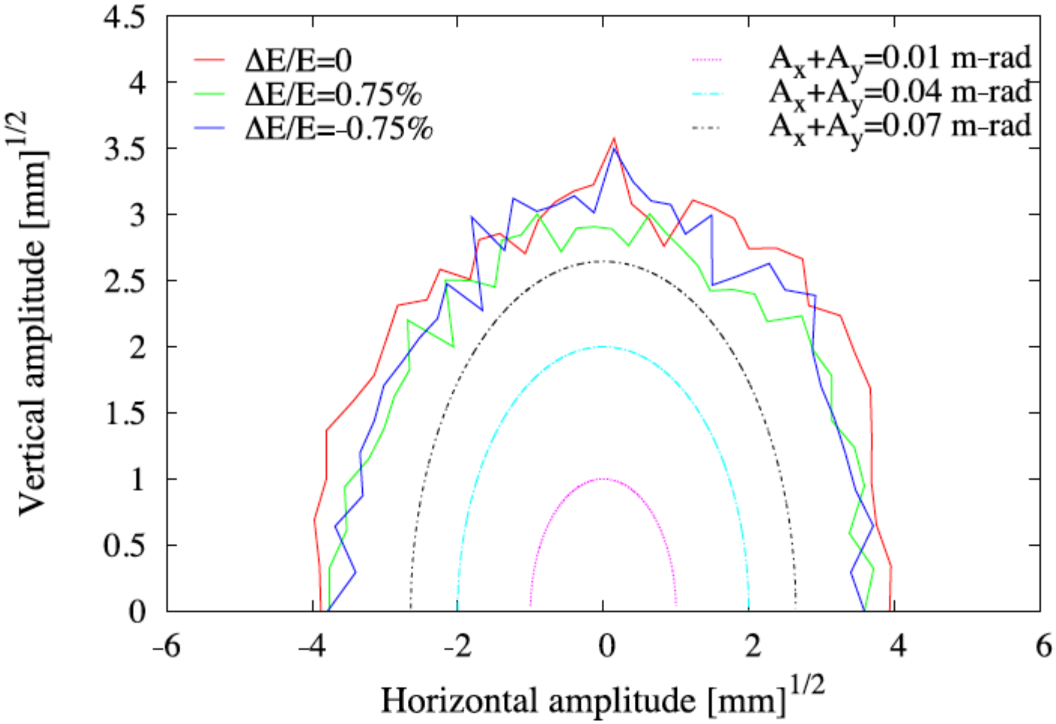

- Dynamic aperture for lattice with specified misalignments, multipole errors, and wiggler nonlinearities
- Specification for the phase space distribution of the injected positron bunch is an amplitude of **A**x + **A**y = 0.07m rad (normalized) and an energy spread of **E/E** 0.75%
- DA is larger then the specified beam acceptance

Dynamic aperture including damping

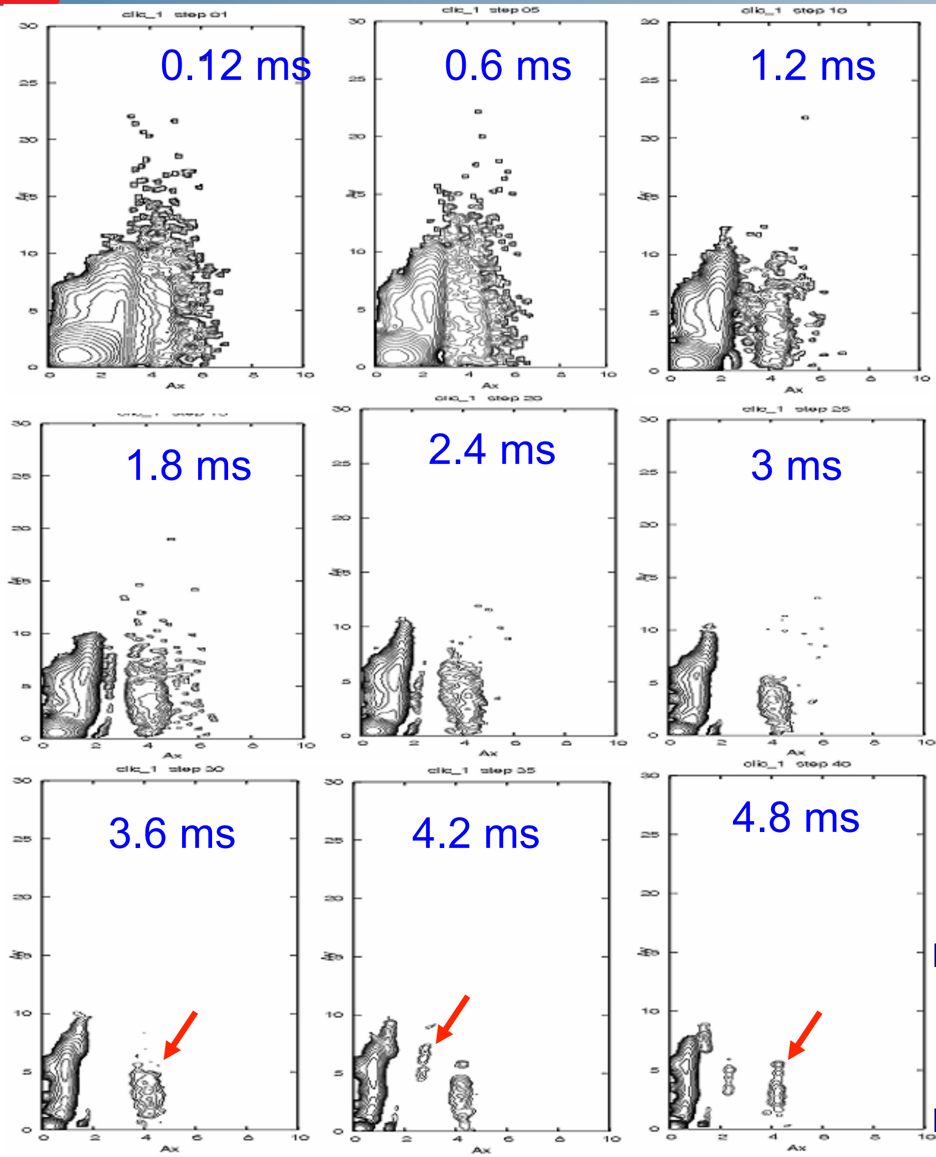

E. Levichev et al. PAC2009

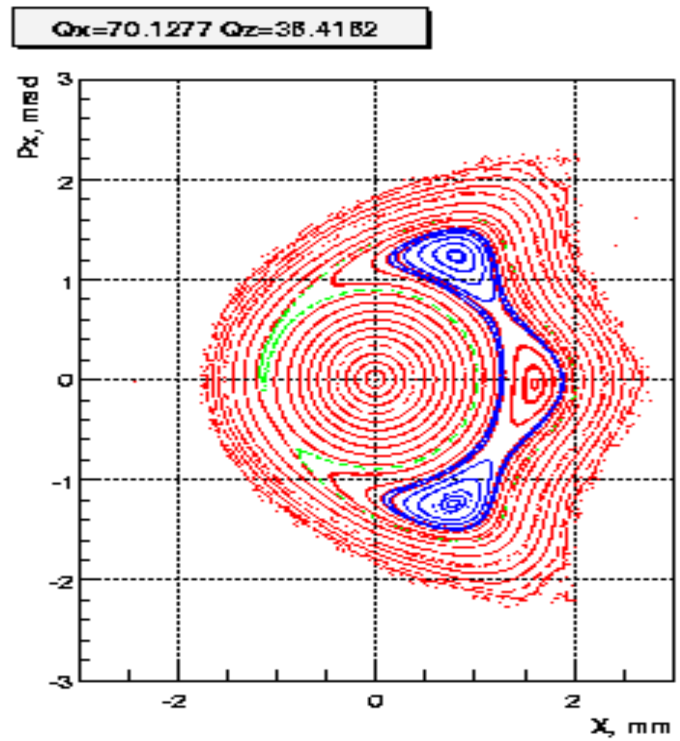

- Including radiation damping and excitation shows that 0.7% of the particles are lost during the damping
- Certain particles seem to damp away from the beam core, on resonance islands

Frequency map analysis

- Frequency Map Analysis (FMA) is a numerical method which springs from the studies of J. Laskar (Paris Observatory) putting in evidence the chaotic motion in the Solar Systems
- FMA was successively applied to several dynamical systems
  - Stability of Earth Obliquity and climate stabilization (Laskar, Robutel, 1993)
  - 4D maps (Laskar 1993)
  - Galactic Dynamics (Y.P and Laskar, 1996 and 1998)
  - Accelerator beam dynamics: lepton and hadron rings (Dumas, Laskar, 1993, Laskar, Robin, 1996, Y.P, 1999, Nadolski and Laskar 2001)

Motion on torus

- Consider an integrable Hamiltonian system of the usual form

$$H(\boldsymbol{J},\boldsymbol{\varphi},\theta) = H_0(\mathbf{J})$$

- Hamilton's equations give

$$\dot{\phi}_j = \frac{\partial H_0(\mathbf{J})}{\partial J_j} = \omega_j(\mathbf{J}) \Rightarrow \phi_j = \omega_j(\mathbf{J})t + \phi_{j0}$$

$$\dot{J}_j = -\frac{\partial H_0(\mathbf{J})}{\partial \phi_j} = 0 \Rightarrow J_j = \text{const.}$$

- The actions define the surface of an invariant torus
- In complex coordinates the motion is described by

$$\zeta_j(t) = J_j(0)e^{i\omega_j t} = z_{j0}e^{i\omega_j t}$$

- For a **non-degenerate** system $\det\left|\frac{\partial\omega(J)}{\partial J}\right| = \det\left|\frac{\partial^2 H_0(J)}{\partial J^2}\right| \neq 0$ there is a one-to-one correspondence between the actions and the frequency, a frequency map can be defined parameterizing the tori in the frequency space

$$F: \quad (\mathbf{I}) \longrightarrow (\omega)$$

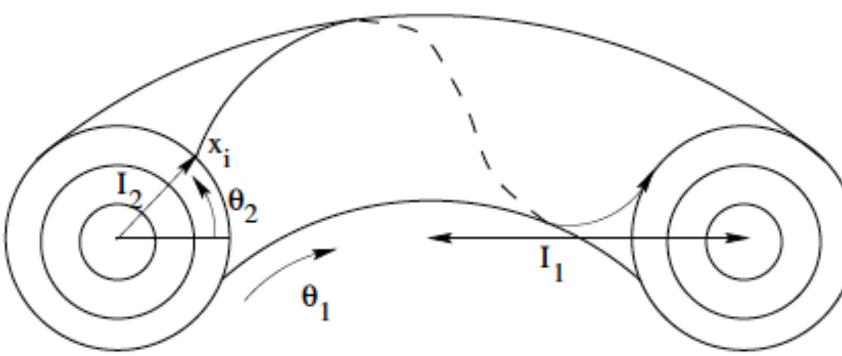

Building the frequency map

- When a quasi-periodic function $f(t) = q(t) + ip(t)$ in the complex domain is given numerically, it is possible to recover a quasi-periodic approximation

$$f'(t) = \sum_{k=1}^{N} a'_k e^{i\omega'_k t}$$

in a very precise way over a finite time span $[-T, T]$ several orders of magnitude more precisely than simple Fourier techniques

- This approximation is provided by the Numerical Analysis of Fundamental Frequencies – **NAFF** algorithm
- The frequencies ω'_k and complex amplitudes a'_k are computed through an iterative scheme.

Aspects of the frequency map

- In the vicinity of a resonance the system behaves like a pendulum
- Passing through the elliptic point for a fixed angle, a fixed frequency (or rotation number) is observed
- Passing through the hyperbolic point, a frequency jump is oberved

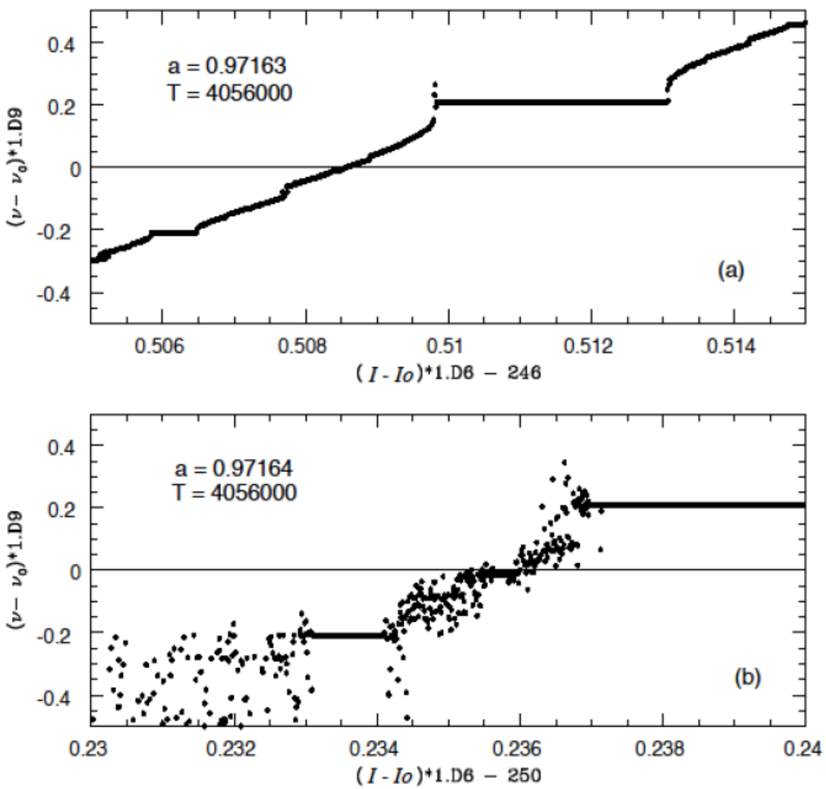

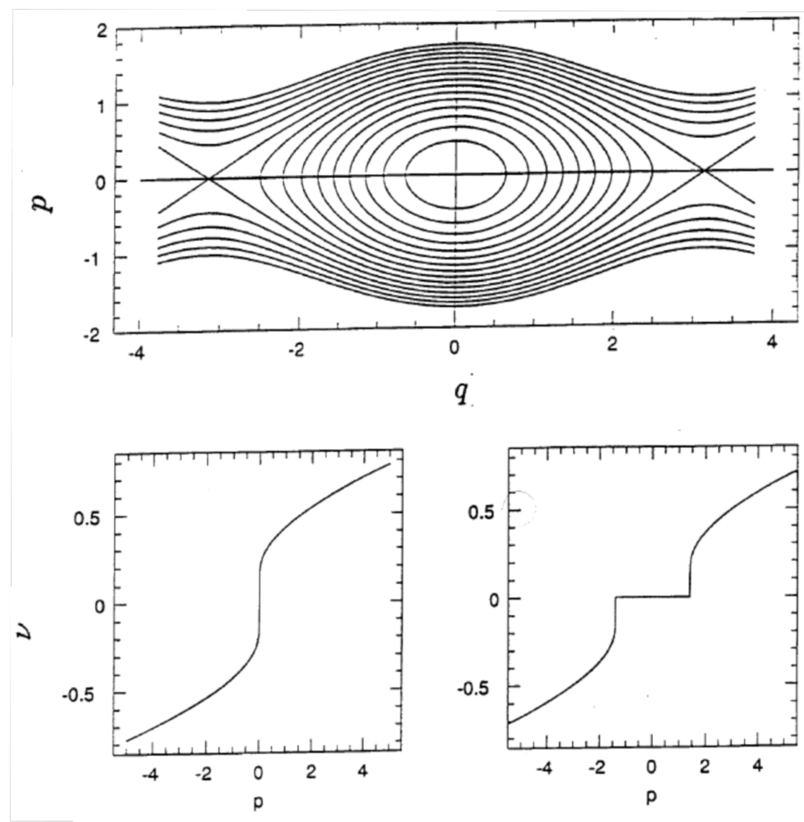

Building the frequency map

- Choose coordinates (x_i, y_i) with p_x and p_y=0
- Numerically integrate the phase trajectories through the lattice for sufficient number of turns
- Compute through NAFF Q_x and Q_y after sufficient number of turns
- Plot them in the tune diagram

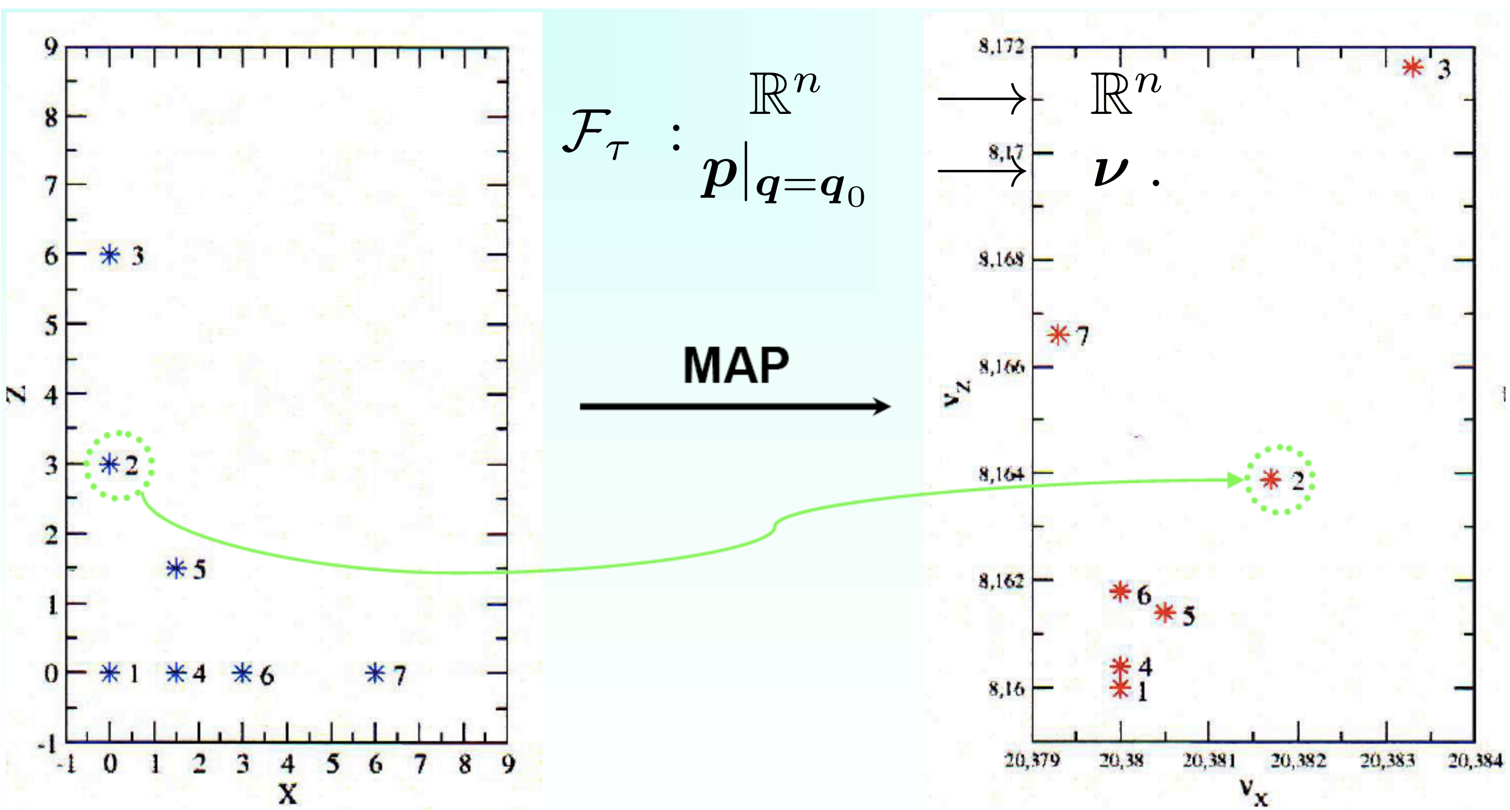

Frequency maps for the LHC

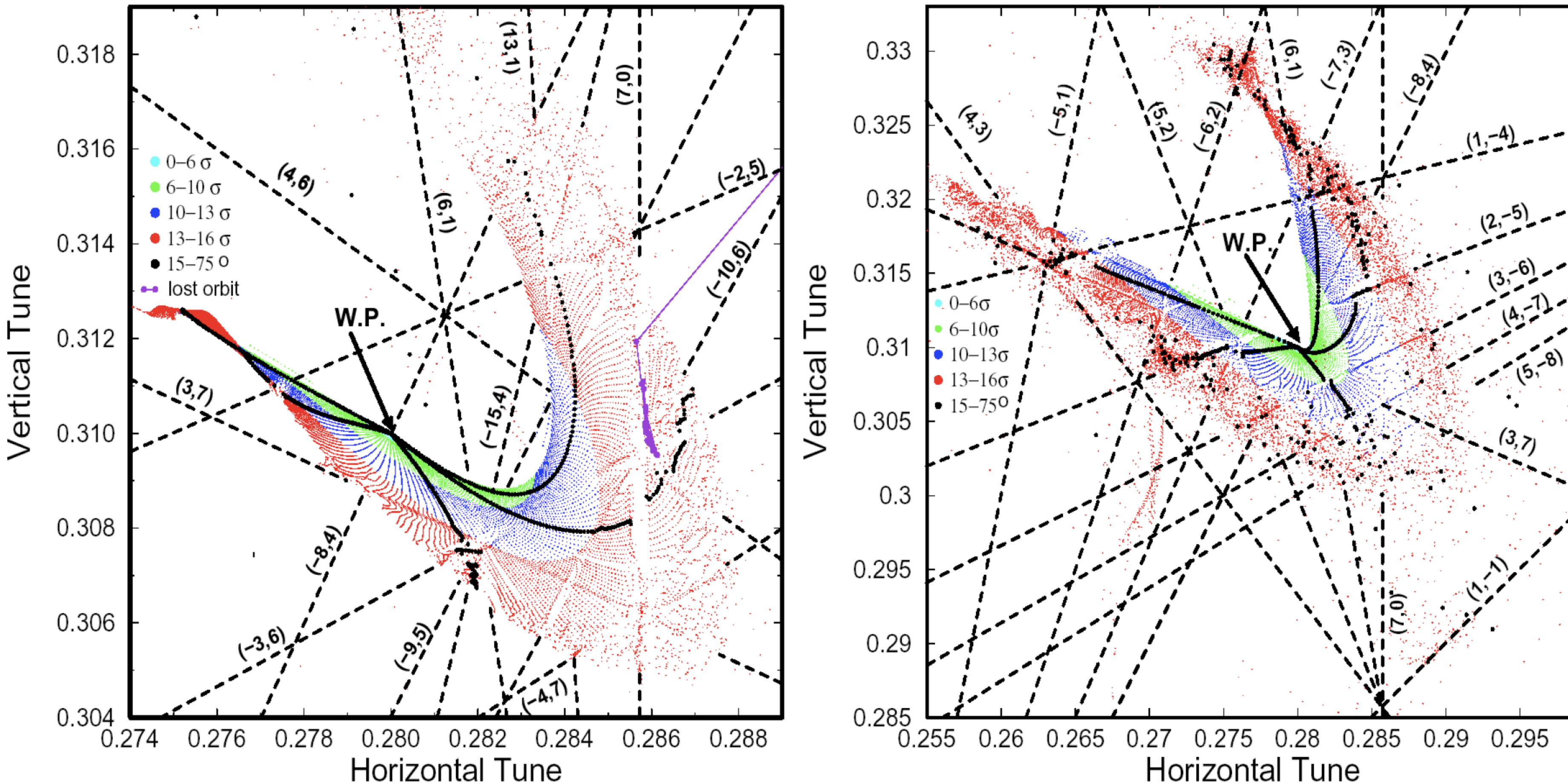

Frequency maps for the target error table (left) and an increased random skew octupole error in the super-conducting dipoles (right)

Diffusion Maps

J. Laskar, PhysicaD, 1993

- Calculate frequencies for two equal and successive time spans and compute frequency diffusion vector:

$$\boldsymbol{D}\big|_{t=\tau} = \boldsymbol{\nu}\big|_{t\in(0,\tau/2]} - \boldsymbol{\nu}\big|_{t\in(\tau/2,\tau]}$$

- Plot the initial condition space color-coded with the norm of the diffusion vector
- Compute a diffusion quality factor by averaging all diffusion coefficients normalized with the initial conditions radius

$$D_{QF} = \left\langle \frac{|\boldsymbol{D}|}{(I_{x0}^2 + I_{y0}^2)^{1/2}} \right\rangle_R$$

Diffusion maps for the LHC

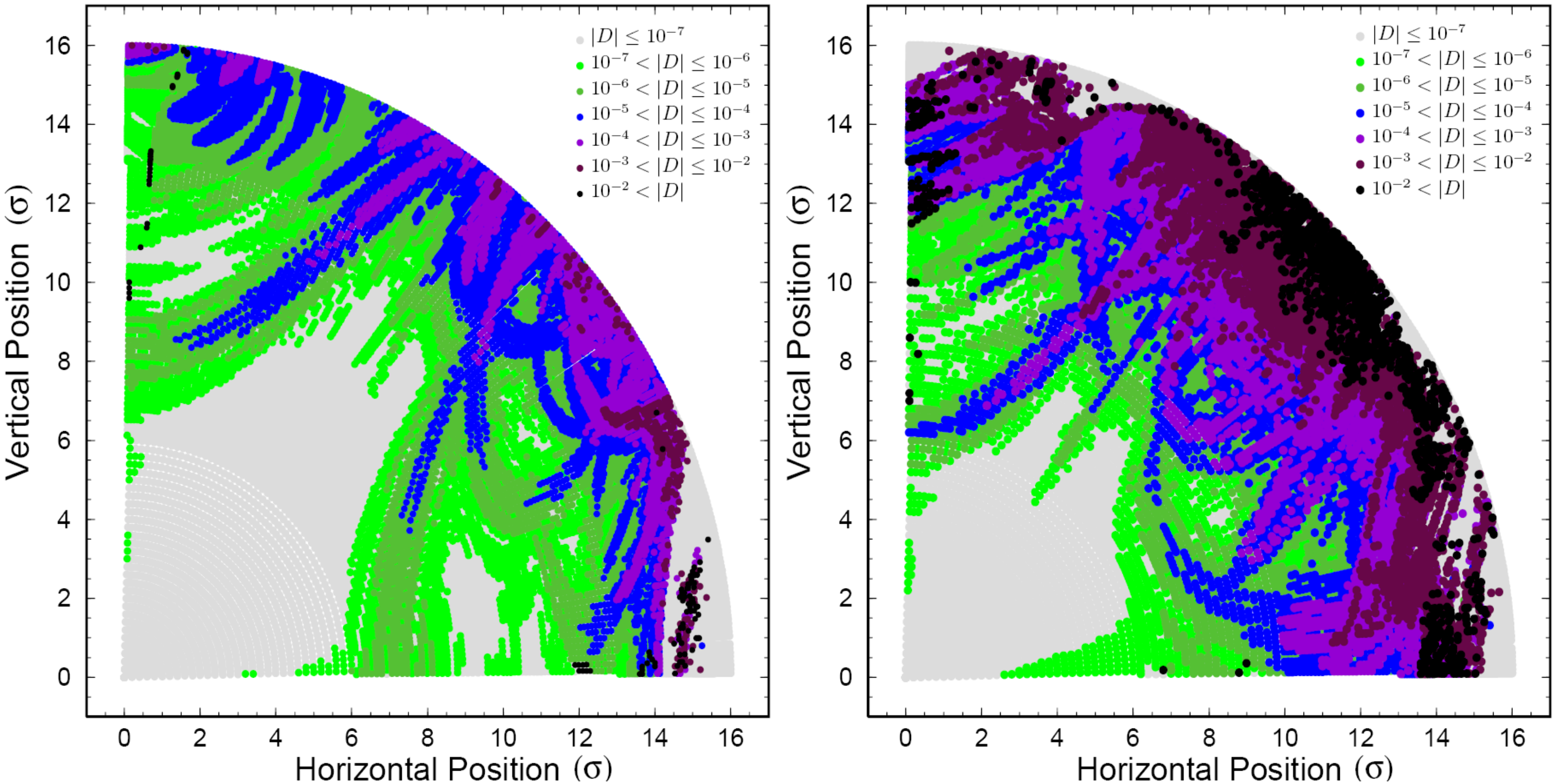

Diffusion maps for the target error table (left) and an increased random skew octupole error in the super-conducting dipoles (right)

- Non linear optimization based on phase advance scan for minimization of resonance driving terms and tune-shift with amplitude

$$\left|\sum_{p=0}^{N_c-1} e^{ip(n_x\mu_{x,c}+n_y\mu_{y,c})}\right| = \sqrt{\frac{1-\cos\left[N_c(n_x\mu_{x,c}+n_y\mu_{y,c})\right]}{1-\cos(n_x\mu_{x,c}+n_y\mu_{y,c})}} = 0$$

⇓

$$N_c(n_x\mu_{x,c}+n_y\mu_{y,c}) = 2k\pi$$

$$n_x\mu_{x,c}+n_y\mu_{y,c} \neq 2k'\pi$$

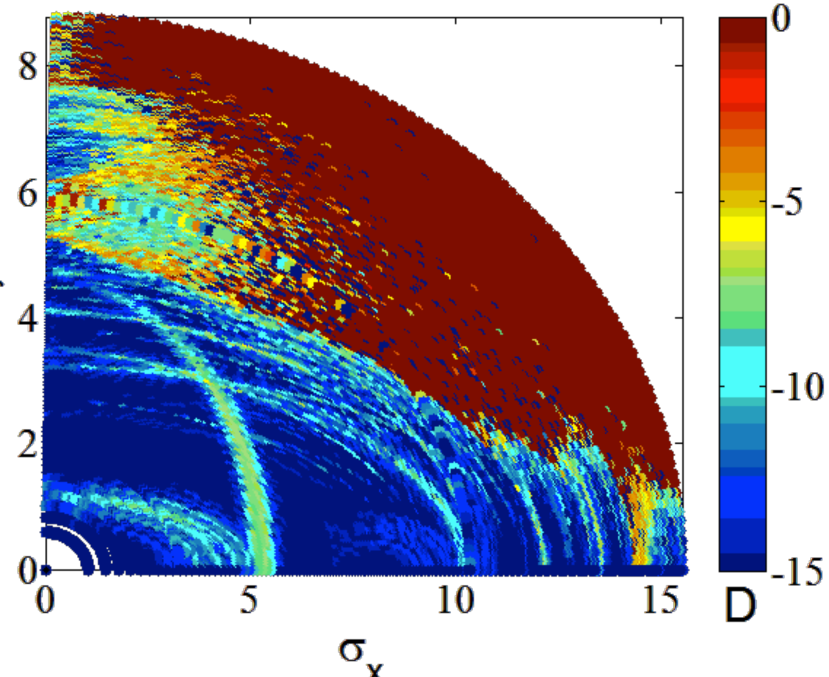

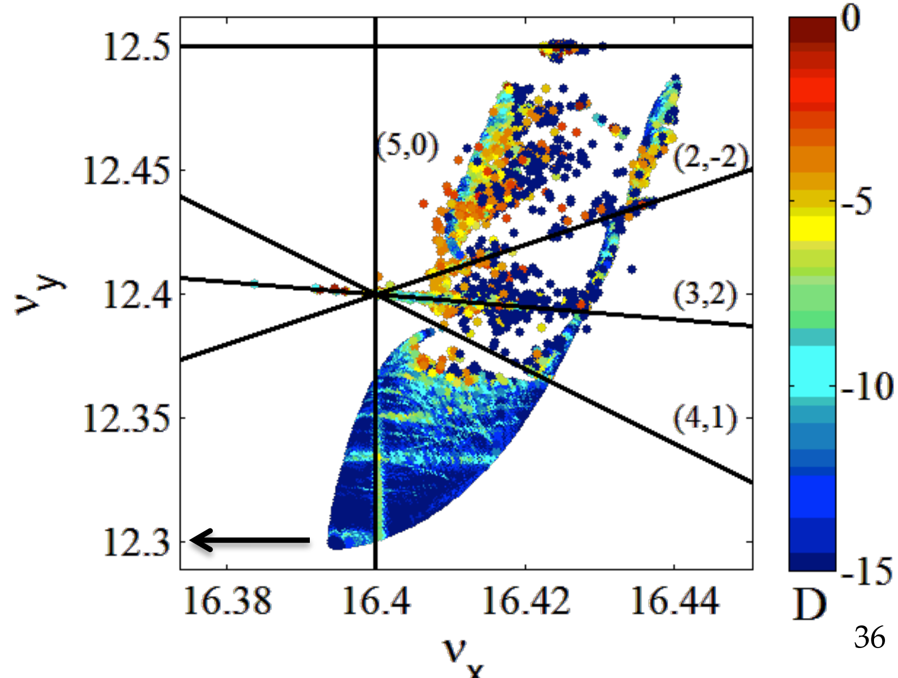

Dynamic aperture for CLIC DR

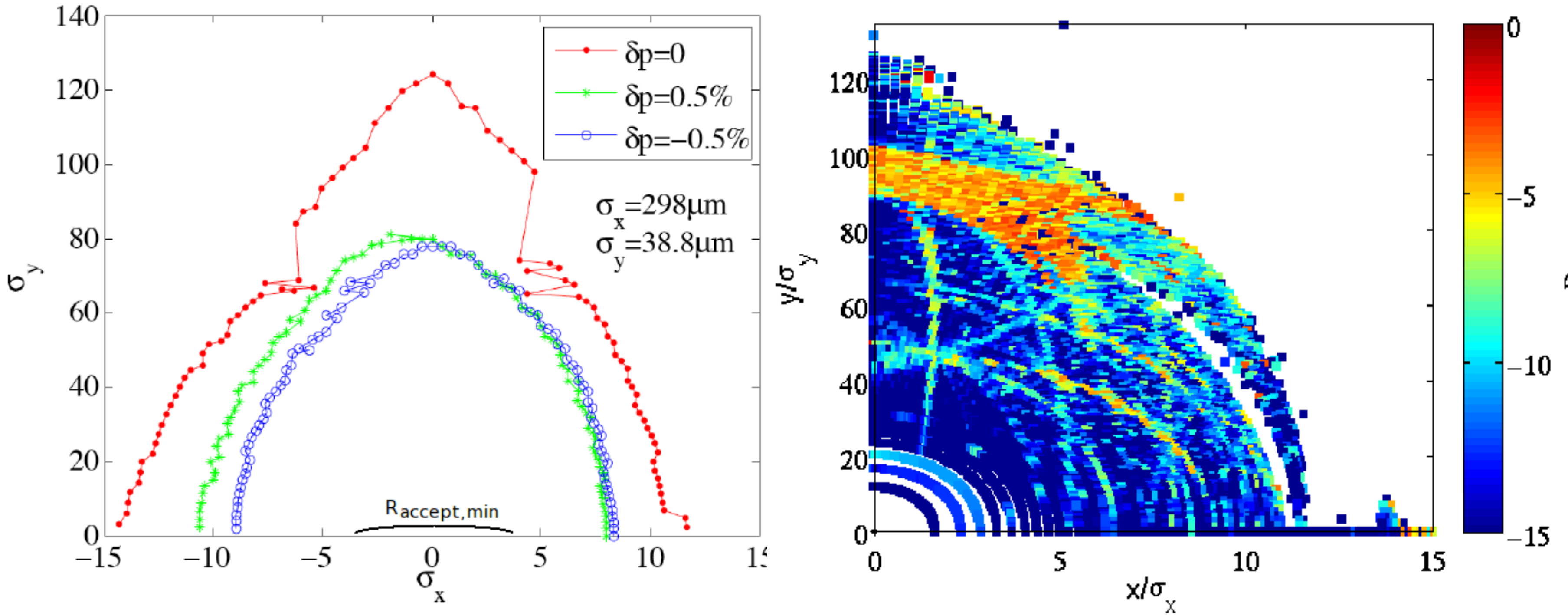

- Dynamic aperture and diffusion map
- Very comfortable DA especially in the vertical plane
  - Vertical beam size very small, to be reviewed especially for removing electron PDR
- Need to include non-linear fields of magnets and wigglers

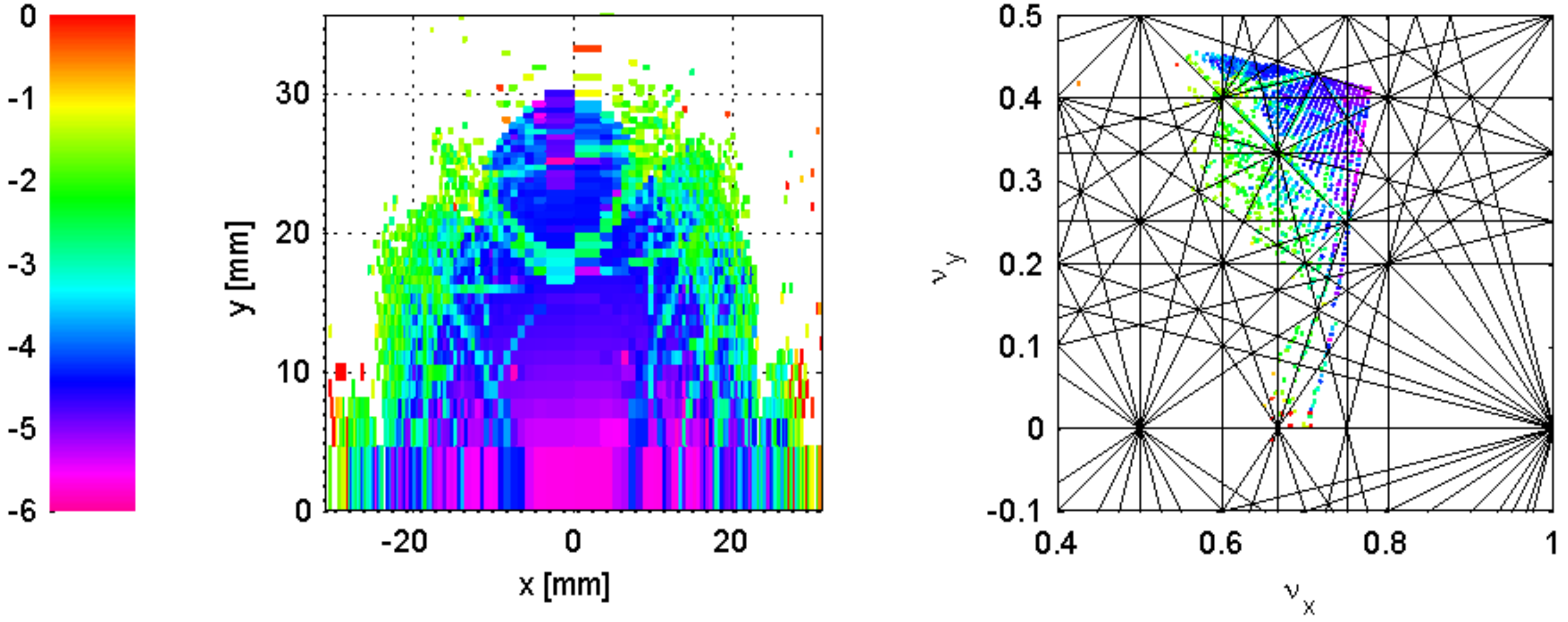

- Frequency maps enabled the comparison and steering of different lattice designs with respect to non-linear dynamics
  - Working point optimisation, on and off-momentum dynamics, effect of multi-pole errors in wigglers

- Figure of merit for choosing best working point is sum of diffusion rates with a constant added for every lost particle
- Each point is produced after tracking 100 particles
- Nominal working point had to be moved towards "blue" area

S. Liuzzo et al., IPAC 2012

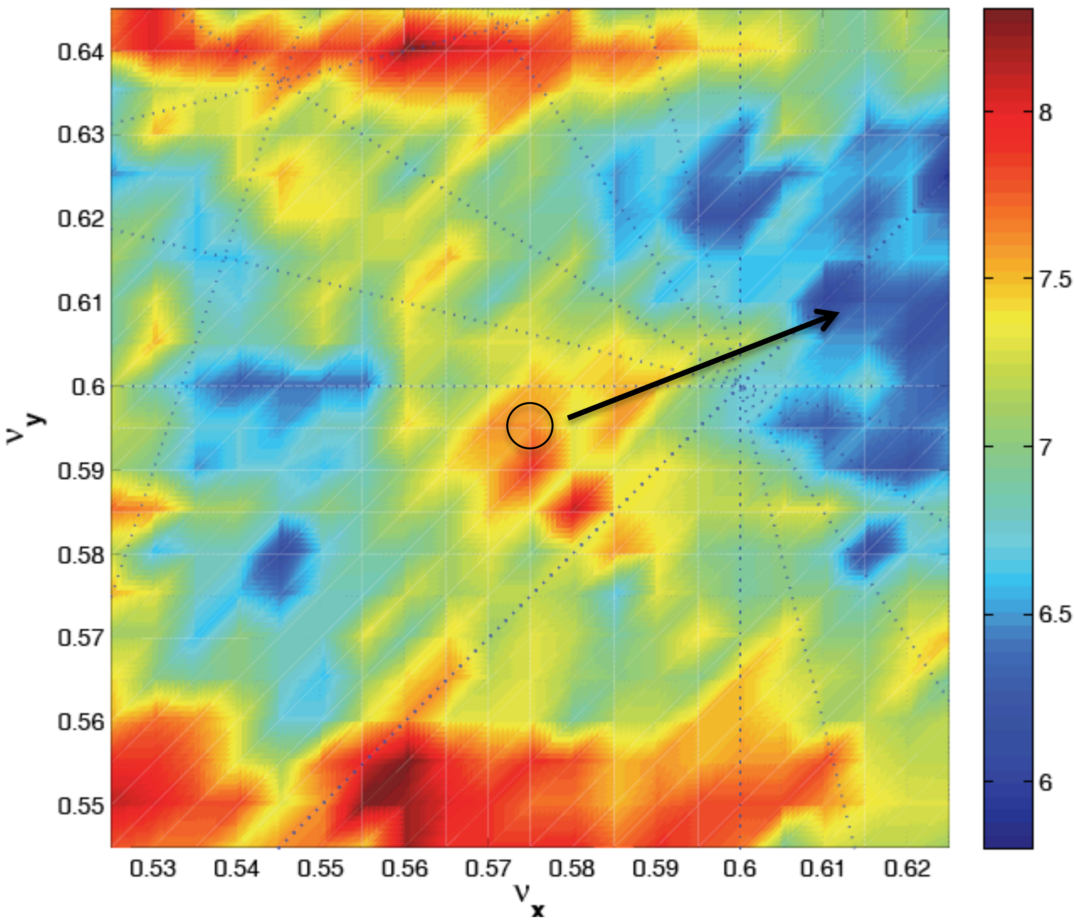

$$e^D = \sqrt{\frac{(\nu_{x,1} - \nu_{x,2})^2 + (\nu_{y,1} - \nu_{y,2})^2}{N/2}}$$

$$WPS = 0.1 N_{lost} + \sum e^D$$

Experimental frequency maps

D. Robin, C. Steier, J. Laskar, and L. Nadolski, PRL 2000

- Frequency analysis of turn-by-turn data of beam oscillations produced by a fast kicker magnet and recorded on a Beam Position Monitors
- Reproduction of the non-linear model of the Advanced Light Source storage ring and working point optimization for increasing beam lifetime

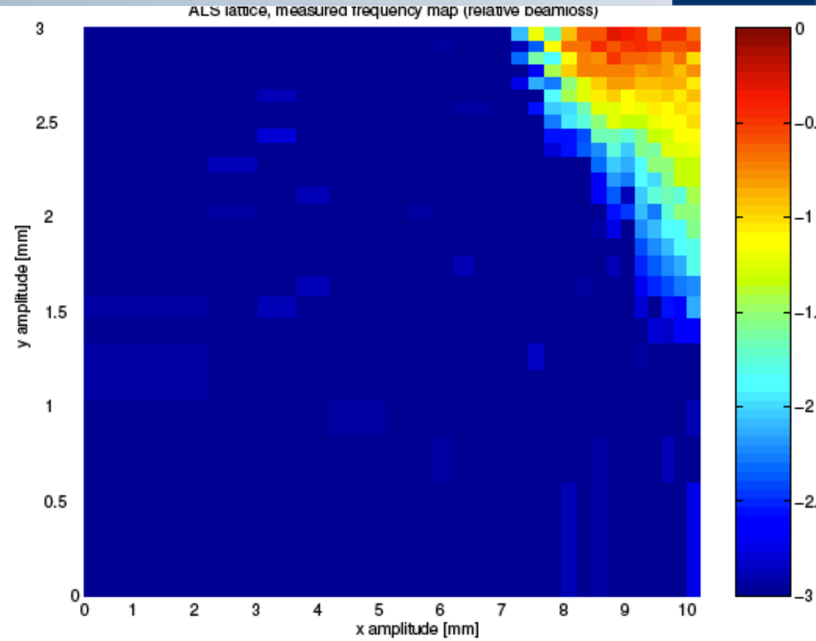

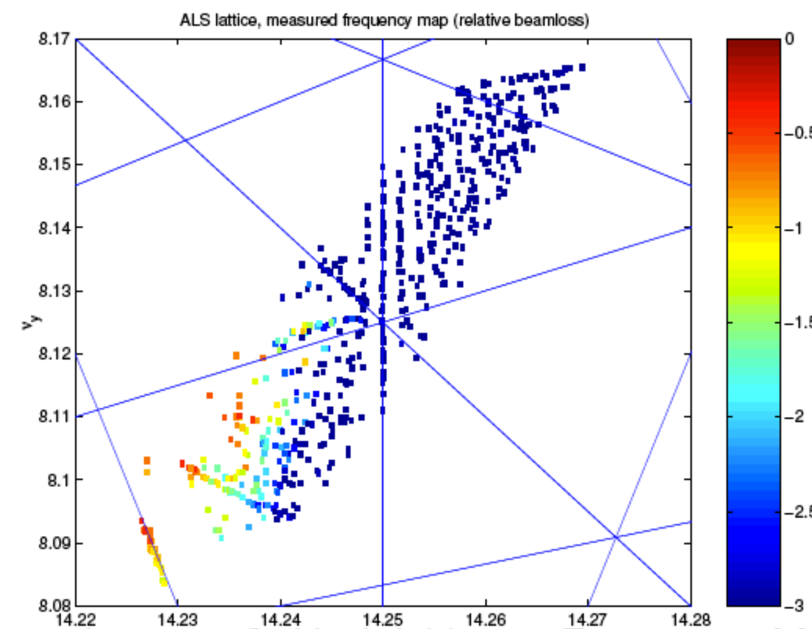

Summary

- Damping rings non-linear dynamics is dominated by very strong sextupoles used to correct chromaticity
- Important effect of wiggler magnets
- Dynamic aperture computation is essential for assuring good injection efficiency in the damping rings
- Frequency map analysis is a very well adapted method for revealing global picture of resonance structure in tune space and enable detailed non-linear optimisation